韓國鑛物學會誌 第 4 卷 第 2 號(1991)
J. Miner. Soc. Korea, 4, 69-89(1991)

Differentiation of the Plutonic Rocks in Saengcho-myon, Sancheong-gun: Trace Element Modelling for the Magmatic Differentiation

산청군 생초면 일대에 분포한 심성암체의 분화에 관한 연구: 마그마분화의 미량원소 모델링

Ji-Gon Jeong(정지곤) · Won-Sa Kim(김원사) · Byong-Min Seo(서병민)

Department of Geology, Chungnam National University, Taejon 305-764, Korea
(충남대학교 지질학과)

ABSTRACT: The anorthositic rocks and the many other plutons which are of different varieties and age were distributed in the northern extremity of the distributed areas of H-S anorthositic rocks. The purpose of this study was to find plutons which had comagmatic relationships, and to make clear the magmatic process of anorthositic magma. The plutons were classified, and the petrological and the geochemical characteristics of the plutons were compared and researched in this study. And, because, like anorthosite, the rocks which intrude in the deep crust accompany assimilation, an AFC model calculation was performed to make the differentiation process of the anorthositic rocks clear.

The plutons in this area were classified into three groups, and the three groups were composed of the Precambrian anorthositic rocks and related rocks, the Jurassic gabbro, and the plutons of unknown age. The anorthositic magma was differentiated from the anorthositic rocks through the tonalite to the alkali-feldspar granite, and it was differentiated under K, Mg, Fe free/lack condition. It was found from the result of AFC model that the anorthositic rocks were differentiated by fractional crystallization, but they were assimilated with wall-rocks, and the assimilation was performed at the rate of $r \leq 0.1$.

The plutons which intruded the anorthositic rocks subsequently consisted of the gabbro, the megacrystic granite, the fine-grained granite, and the gneissose granite. But they were formed by the repeated intrusion of magma, which may, or may not, be of the same origin. According to the result of the RCF model, these plutons were differentiated by simple fractional crystallization, and they were assimilated relatively less than the anorthositic rocks.

요약: 하동-산청지역에 분포되어 있는 회장암질암 분포지역의 최북단에는 회장암질암을 비롯하여 종류와 시기가 다른 여러가지 관입암체가 분포되어 있다. 본 연구는 이들 여러 종류의 관입암체들과 회장암의 시기적, 성인적 관계유무를 밝혀 회장암과 동원의 마그마에 기원을 둔 암체를 찾고 회장암질암의 분화과정을 밝혀내는 데 목적을 두었으며 위의 목적을 수행하기 위하여 암체의 분류, 암석학적 및 지화학적 특징 등을 비교 연구하였다. 그리고 회장암과 같은 심부에서 관입한 암체는 주변암체와의 심한 동화작용을 수반하기 때문에 회장암질암의 분화과정을 알아보기 위하여 AFC 모델계산 등을 시행하였다.

본 연구지역에 분포되어 있는 심성암체는 회장암질암과 관련암체, 그리고 쥬라기의 반려암과 시대미상의 심성암체로 대분된다. 회장암질암은 회장암질암→토날라이트→알카리장석 화강암으로 분화되었으며 K, Mg, Fe 성분이 매우 결핍 혹은 고갈된 환경하에서 분화되었다. AFC 모델에 의하면 회장암질암은 분별결정작용에 의해 분화되었으나 주변암체와 심하게 동화되었고 동화작용은 $r \leq 0.1$ 의 속도로 진행되었다.

후기에 회장암질암을 관입한 심성암체는 반려암, 거정질 반상화강암, 세립질화강암, 편마상화강암 등이며 반려암과 화강암류는 기원이 같거나 혹은 다른 마그마의 반복적인 관입에 의해 형성되었다. RCF 모델에 의하면 이들 암체는 분별정출작용에 의해 결정화 되었으며 회장암질암에 비해 비교적 적은 양의 동화작용을 수반하였다.

INTRODUCTION

The studied areas were some parts of Saengcho-myon and of Sudong-myon, Sancheong-gun, the northern extremity of the distributed areas of the H-S Anorthositic rocks (Fig. 1). Geological maps of the studied area, the Sancheong sheet (Kim et al., 1964) and the Aneui sheet (Hwang and Park, 1968), were previously published by the Geological Survey of Korea. Son and Jeong (1972), Jeong (1980, 1982, 1987), Jeong and Lee (1986), and Kwon and Jeong (1990) had previously researched the origin, the differen-tiation, and the metamorphism of the anorthositic rocks (hereafter AnRs) in this district.

In case of the other countries, the anorthosites of the skaergaard Intrusion (Wager and Brown, 1967) and of the Nain anorthosite series (Morse, 1968) were differentiated along with other rocks which had different chemical compositions. Consequently, it is theoretically possible that the AnRs in this area originally contained their related rocks.

The purpose of this study was to make clear the relationships between the AnRs and the other plutons, and to find the rocks which had comagmatic relationships with AnRs. To achieve the purpose, the plutons were classified, and the petrological and the geochemical characteristics of the plutons were compared and studied.

GENERAL GEOLOGY AND PETROGRAPHY

The studied area was mainly composed of the Precambrian migmatitic gneiss and the plutons which intruded it, the basic dykes of unknown age, the Jurassic gabbro which intruded the AnRs, and the plutons also of unknown age (Fig. 1). The Precambrian plutons were composed of the AnRs, the tonalite, which had gradational relationships with the AnRs, and the alkali-feldspar granite (hereafter AfGr) which intruded the AnRs. The basic dykes of unknown age intruded the AnRs in all parts of the distributed area of the AnRs. The plutonic rocks of unknown age intruded all of the rocks explained above, and these were composed of the megacrystic granite (hereafter MGr), the fine-grained granite (hereafter FgGr), and the gneissose granite (hereafter GnGr) which had gradational relationships one another.

A fault existed along the valley which was formed west of Saengcho (Fig. 1). The broken boundary lines were evidence of the fault, but other evidence could not be found in the field. Since the fault broke the boundary lines of the GnGr, it is reasonable to infer that the age of the fault is younger than that of the GnGr. The modal composition of the plutons are shown in Table 1, and the characteristics observed in the field and under the microscope are the same as below.

Table 1. Modal composition of the plutonic rocks in Saengcho area (vol.%)

	Anorthositic rock													
	29-29	29-25	29-12	I-7	I-4	OB29-2	0B27-3	Ap27-4	OB27-2	OB29-4	Feb16-4	Feb14-6	Ap29-5	Feb17-7
Quartz	4.2	5.8	4.2	-	1.5	0.5	-	1.6	1.6	0.6	tr	1.4	1.8	1.3
Plagioclase	91.8	92.2	94.8	97.1	94.2	96.8	97.4	96.3	75.2	56.5	68.1	89.8	97.0	94.7
Orthopyroxene	-	-	-	-	-	-	-	-	-	-	-	-	-	-
Clinopyroxene	-	-	-	-	-	-	-	-	-	-	-	-	-	-
Hornblende	-	0.3	-	0.7	1.7	0.9	1.7	tr	22.0	42.5	27.8	7.1	tr	-
Tr & Ac	-	-	-	1.1	2.0	-	-	-	1.2	tr	4.1	tr	-	-
Biotite	tr	0.1	-	1.1	-	-	0.3	tr	-	-	-	-	0.2	-
Opaque	0.1	tr	tr	tr	tr	0.8	tr	tr	tr	0.4	tr	0.3	tr	tr
Chlorite	0.1	0.2	tr	tr	0.2	0.8	0.5	1.1	tr	tr	tr	1.0	0.8	0.3
Calcite	0.8	0.5	tr	-	-	-	-	-	tr	tr	-	tr	-	-
Epidote	tr	0.3	0.5	tr	0.4	tr	0.1	0.2	tr	tr	-	0.4	0.1	1.2
Muscovite	3.0	0.6	0.5	tr	-	0.2	tr	0.8	-	-	-	tr	0.1	2.5
Zircon	tr	-	-	-	-	-	-	-	-	-	-	-	tr	-
Total	100.0	100.0	100.0	100.0	100.0	100.0	100.0	100.0	100.0	100.0	100.0	100.0	100.0	100.0

Tr & Ac: tremolite & actinolite, tr: trace

Table 1. (continued)

	Anorthositic rock								Tonalite			Alkali-feldspar granite		
	Feb14 -1	Feb14 -8	Feb15 -3	Feb15 -4	Feb14 -9	Feb15 -7	Feb15 -11	Feb15 -9	Ap29 -2	Ap29 -6	Sp7-1	24-2	5-1-1	WR
Quartz	-	-	-	-	0.1	-	-	tr	29.3	32.4	19.0	43.4	46.3	51.2
Orthoclase	-	-	-	-	-	-	-	-	-	-	tr	12.8	9.8	11.5
Microcline	-	-	-	-	-	-	-	-	-	-	-	30.5	37.4	31.0
Plagioclase	98.9	96.6	94.4	97.0	96.9	95.1	98.2	85.4	69.8	61.0	70.2	12.6	6.5	5.5
Orthopyroxene	-	-	-	-	-	-	-	-	-	-	-	-	-	-
Clinopyroxene	-	-	-	-	-	-	-	-	-	-	-	-	-	-
Hornblende	-	2.5	2.2	tr	1.8	-	0.7	11.3	tr	4.5	-	-	-	-
Tr & Ac	-	0.2	1.9	-	tr	2.7	-	tr	-	-	5.1	-	-	-
Biotite	-	-	0.2	-	-	0.8	-	-	tr	-	-	0.5	tr	0.8
Opaque	tr	0.4	0.1	tr	0.2	tr	tr	tr	tr	tr	-	tr	tr	-
Chlorite	0.3	0.3	0.9	1.7	1.0	1.4	1.1	1.9	0.6	0.9	2.9	tr	-	tr
Calcite	-	-	tr	1.1	-	-	-	tr	-	-	-	-	-	-
Epidote	tr	tr	-	0.2	tr	-	tr	1.4	tr	0.1	tr	-	-	-
Muscovite	0.8	-	0.3	-	-	-	-	-	0.3	1.1	2.8	0.2	tr	-
Zircon	-	-	-	-	-	-	-	-	-	tr	-	tr	-	-
Total	100.0	100.0	100.0	100.0	100.0	100.0	100.0	100.0	100.0	100.0	100.0	100.0	100.0	100.0

Tr & Ac: tremolite & actinolite, tr: trace

Table 1. (continued)

	Gabbro						Megacrystic granite					
	OB29 -1	OB29 -5	OB27 -6	OB27 -7	Feb16 -3	Feb16 -5	I-10	0B28 I-5	OB29 -11	30-3	30-7	Feb17 -1
Quartz	0.8	1.2	tr	tr	0.7	1.0	28.6	29.8	26.3	39.5	40.3	25.3
Orthoclase	-	-	-	-	-	-	7.6	5.8	12.9	9.8	12.2	8.4
Microcline	-	-	-	-	-	-	16.1	15.1	17.3	18.1	2.5	21.8
Plagioclase	34.4	37.7	49.1	50.3	36.6	35.4	46.2	40.7	36.3	26.2	26.7	38.3
Orthopyroxene	-	-	8.9	6.7	-	-	-	-	-	-	-	-
Clinopyroxene	-	-	9.3	13.4	-	24.2	-	0.2	-	-	-	-
Hornblende	56.1	48.2	23.2	21.7	47.4	29.6	0.4	1.0	0.3	-	9.0	-
Tr & Ac	-	-	-	1.2	-	-	-	-	-	-	-	-
Biotite	6.1	8.4	4.1	3.8	9.1	6.4	0.8	6.4	5.5	5.4	7.0	3.8
Opaque	2.6	3.1	0.8	0.4	2.5	1.0	tr	0.1	0.1	tr	tr	0.3
Chlorite	tr	1.4	4.6	2.5	3.7	2.4	0.2	0.9	1.1	0.5	1.5	1.4
Calcite	-	-	-	tr	-	-	-	tr	tr	-	-	0.7
Epidote	-	tr	-	-	-	tr	0.1	tr	0.1	-	0.4	tr
Muscovite	-	-	-	-	-	-	-	-	-	-	0.4	-
Zircon	-	-	-	-	-	-	-	tr	tr	tr	-	tr
Sphene	-	-	-	-	-	-	-	-	-	0.5	-	-
Garnet	-	-	-	-	-	-	-	-	-	-	-	-
Total	100.0	100.0	100.0	100.0	100.0	100.0	100.0	100.0	100.0	100.0	100.0	100.0

Tr & Ac: tremolite & actinolite, tr: trace

Table 1. (continued)

	Megacrystic granite		Gneissose granite									
	30-4	2-9	Ma20 -4	De12 -4	Ap28 -5	Ap29 -8	De12 -6	Ap28 -4	Ma20 -7	Ma1 -1	De12 -5	Ap26 -2
Quartz	35.6	34.2	46.8	47.0	40.0	49.0	42.1	48.6	48.1	51.0	40.5	43.4
Orthoclase	6.9	10.6	10.0	4.4	11.3	3.4	10.3	15.6	5.2	7.3	11.8	13.1
Microcline	20.0	13.8	13.3	24.3	15.2	27.4	20.9	11.0	21.5	15.0	29.0	18.1
Plagioclase	30.4	32.7	21.3	22.8	32.5	18.7	20.6	18.1	23.8	12.3	17.8	20.9
Orthopyroxene	-	-	-	-	-	-	-	-	-	-	-	-
Clinopyroxene	tr	tr	-	-	-	-	-	-	-	-	-	-
Hornblende	0.4	0.2	-	-	-	-	-	-	-	-	-	-
Tr & Ac	-	-	-	-	-	-	-	-	-	-	-	-
Biotite	3.6	7.4	7.8	0.8	0.8	0.9	4.5	5.4	1.4	9.7	tr	2.9
Opaque	0.2	0.3	0.2	0.5	0.1	0.3	tr	0.8	tr	0.9	0.7	0.7
Chlorite	1.6	0.6	0.6	0.1	0.1	0.3	1.3	0.5	tr	1.2	0.2	0.9
Calcite	tr	tr	-	-	-	-	-	-	-	-	-	-
Epidote	0.1	0.2	-	tr	-	-	tr	-	-	-	-	tr
Muscovite	1.2	tr	tr	0.1	tr	tr	0.3	tr	tr	2.6	-	tr
Zircon	tr	tr	tr	-	-	-	tr	-	tr	tr	-	-
Sphene	-	-	-	-	-	-	-	-	-	-	-	-
Garnet	-	-	tr	-	-	-	-	-	-	-	-	tr
Total	100.0	100.0	100.0	100.0	100.0	100.0	100.0	100.0	100.0	100.0	100.0	100.0

Tr & Ac: tremolite & actinolite, tr: trace

Table 1. (continued)

	Fine-grained granite								
	Ap27 -3	Ap28 -2	Feb16 -8	Feb17 -3	Feb17 -4	Feb17 -6	OB29 -8	OB29 -6	OB29 -9
Quartz	38.4	43.5	36.9	51.1	50.5	48.4	53.4	40.5	43.6
Orthoclase	2.1	4.5	3.3	1.0	3.6	2.4	-	6.7	16.0
Microcline	24.5	20.6	18.4	32.3	31.6	29.5	21.6	13.8	10.9
Plagioclase	28.5	26.2	32.1	13.9	13.5	17.7	21.0	31.9	25.9
Orthopyroxene	-	-	-	-	-	-	-	-	-
Clinopyroxene	-	-	-	-	-	-	-	-	-
Hornblende	-	-	tr	-	-	-	tr	-	-
Tr & Ac	-	-	-	-	-	-	-	-	-
Biotite	4.0	3.1	6.4	0.3	0.7	1.0	3.4	4.5	2.4
Opaque	tr	0.6	0.8	1.2	tr	tr	tr	0.4	0.7
Chlorite	1.8	0.3	2.1	tr	tr	0.7	0.3	0.5	tr
Calcite	-	-	-	-	-	-	-	-	-
Epidote	-	-	tr	-	-	-	0.3	-	-
Muscovete	0.7	1.2	tr	0.2	0.1	0.3	-	1.7	0.5
Zircon	tr	tr	tr	tr	-	-	-	tr	-
Sphene	-	-	-	-	-	-	-	-	-
Garnet	-	-	-	-	-	-	-	-	-
Total	100.0	100.0	100.0	100.0	100.0	100.0	100.0	100.0	100.0

Tr & Ac: tremolite & actinolite, tr: trace

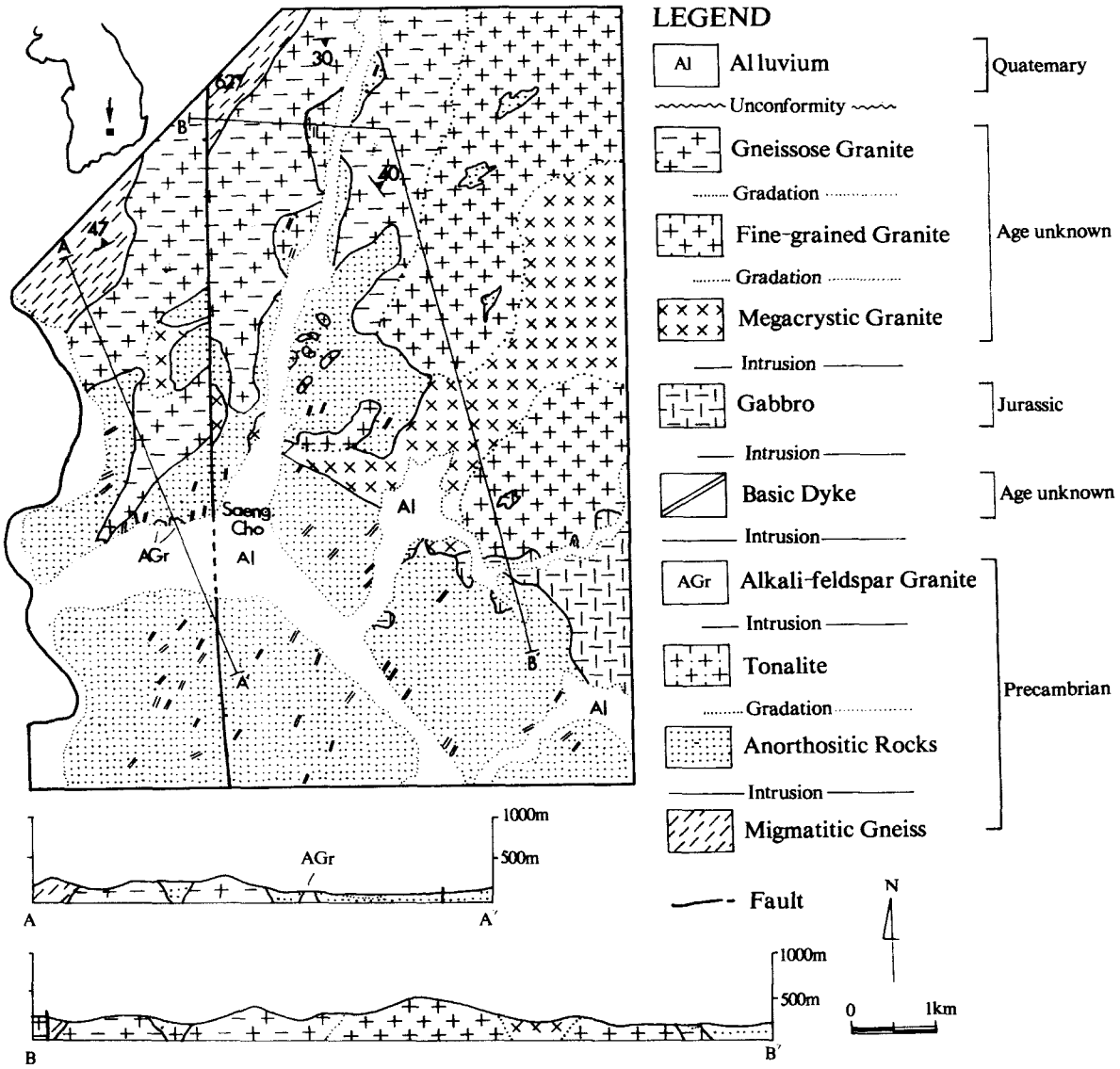

Fig. 1. Geologic map of the area studied.

Migmatitic gneiss

The migmatitic gneiss was the basement of the studied area, and was distributed in the northwestern parts of the area, and was intruded by the AnRs. Because of the dark green bands which were mainly composed of biotite and hornblende, it was distinguished easily from the other rocks. The grain size was from fine to medium (0.5~2mm), and it showed the texture that the marginal parts of the minerals had been remelted.

Anorthositic rocks

The intrusion age of the AnRs which were distributed in the southern half of the studied area was 1.7 b.y. (Kwon and Jeong, 1990), and it was affected by the latest retrogressive metamorphism which acted on the Sobaeksan massif three times (Jeong and Lee, 1986). The AnRs were intruded by the basic dykes and the other plutons, but they had gradational relationship with the tonalite.

The AnRs in the field showed a white color,

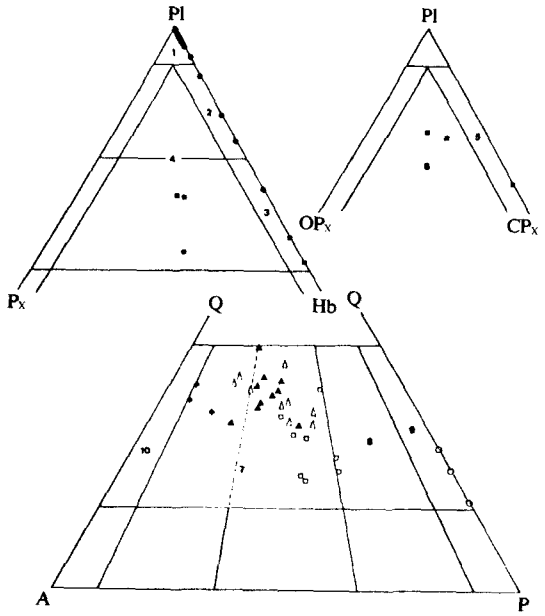

Fig. 2. Triangular diagram of modal composition for the plutonic rocks.
1: Anorthosite; 2: Leuco-hornblende gabbro; +3: Hornblende gabbro; 4: Pyroxene-hornblende gabbro/norite 5: Gabbro; 6: Gabbronorite; 7: Granite; 8: Granodiorite; 9: Tonalite; 10: Alkali-feldspar granite;
● : Anorthosite; ■ : Gabbro; ○ : Tonalite;
◆ : Alkali-feldspar granite;
□ : Megacrystic granite;
△ : Fine-grained granite; ▲ : Gneissose granite

because they rarely contained mafic mineral. But some of them had a lot of mafic mineral (≤40%), although they did not follow rigorous rule (Table 1). They had euhedral or subhedral equigranular grains (1~3.5mm), and were plotted in the field of anorthosite and leuco-hornblende gabbro in the triangular diagram of plagioclase-pyroxene-hornblende (hereafter Pl-Px-Hb) (Fig. 2).

Tonalite

The tonalite was distributed in the northern extremity of the area of the AnRs, and had gradational relationship with the AnRs, and the relationship showed that the amount of quartz in AnRs increased gradually, and became tonalite. The tonalite was intruded by the basic dykes and the GnGr. In the field, it was very difficult to distinguish tonalite from the AnRs because it showed a white color, and because it had a similar color in weathered outcrops. But it was thought that the rocks which crystallized in the late stage of the differentiation of anorthositic magma remained after the intrusion of the GnGr. It had subhedral or anhedral equigranular grains (0.8~3.5mm), and belonged to the field of the tonalite in the triangular diagram of quartz-alkali feldspar-plagioclase (hereafter Q-A-P) (Fig. 2).

Alkali-feldspar granite

The AfGr was distributed in a small area (Fig. 1) 500 meters west of Saengcho. It showed a white color that was very similar to that of the AnRs, and intruded the AnRs. Under microscope, it showed the texture that the marginal part of the crystals, such as quartz and feldspar, were crushed, and had subhedral to anhedral equigranular grains (0.8~3mm). It was plotted in the field of syenogranite in the Q-A-P triangular diagram (Fig. 2).

Basic dykes

The basic dykes were observed in all the distributed areas of the AnRs, and intruded the AnRs, the tonalite, and the AfGr, among the many other plutons distributed in the studied area. The direction of intrusion was N10~60° E, 50~85° SE, and it had 30Cm~3m width. In some parts, foliation had grown parallel to the direction of intrusion. It was mainly composed of plagioclase, hornblende, and small amounts of quartz and biotite.

Gabbro

The gabbro was distributed in southeastern parts of the studied area. The intrusion age, which was measured by the K-Ar method using hornblende, is 169.58±2.57m.y., and this comes under Jurassic. The gabbro had euhedral to subhedral equigranular grains (0.5~3mm), and belonged to the field of pyroxene-hornbelde gabbro/norite and hornblende gabbro in the triangular diagram of Pl-Px-Hb (Fig. 2). Those which belonged to the field of pyroxene-hornblende gabbro/norite were plotted in the field of gabbronorite and

gabbro in the triangular diagram of plagioclase ortho pyroxene-clinopyroxene (Fig. 2).

Megacrystic granite

The MGr, which was distributed in eastern part of the studied area, was named as granodiorite in the Sancheong sheet (Kim et al., 1964) and was named as coarse-grained granitic gneiss in the Aneui sheet (Hwang and Park, 1968). It had gradational relationships with the FgGr and the GnGr. Its megacrysts had various sizes (10~40mm in long diameter, 5~20mm in short diameter), and they were euhedral or subhedral microcline or plagioclase. It was plotted in the field of monzogranite in the triangular diagram of Q-A-P(Fig. 2), and the megacrysts were crushed near the contact with the AnRs.

Fine-grained granite

The FgGr was mainly distributed in northeastern parts of the studied area. It intruded the gabbro, and had gradational relationships with the GnGr and the MGr. It had euhedral to subhedral equigranular grains (0.5~1mm), and was plotted in the vicinity of the boundary between syeno-granite and monzogranite (Fig. 2).

Gneissose granite

The GnGr was distributed broadly in northwestern parts of the studied area. The grain size was 0.5~3mm, and the mafic minerals, such as biotite and hornblende, were arranged in the same direction (N10~40° E, 60~70° SE). Evidence that it intruded the AnRs was found in many places in this area. It had gradational relationships with the MGr and the FgGr. It had subhedral to anhedral equigranular grains, and was plotted in the vicinity of the boundry between syenogranite and monzogranite (Fig. 2). Thus, it was concluded that it had a similar mineral composition with the FgGr.

PETROCHEMISTRY

Twenty-six samples were selected to study the geochemical characteristics of the plutons distributed in the studied area, and major and trace elements were analysed by ICP (ACTIVATION LABORATORIES LTD, ONTARIO, CANADA). The results of analyses were listed in Tables 2, 3, 4, and 5.

Precambrian Plutonic Rocks

The content of K_2O showed an increasing trend from the AnRs through the tonalite to the AfGr, and the contents of TiO_2, Al_2O_3, and CaO showed decreasing trend in the Haker's diagrams (Fig. 6). But the contents of Fe_2O_3* and MgO were maintained low and constantly. Among the major elements which were contained in the AnRs, the contents of Fe_2O_3*, MgO, Na_2O and K_2O were lower than the foreign anorthosites that were already reported (Letteney, 1968, Herz, 1968, Green, 1968). But the contents of Al_2O_3 and CaO were higher than those of the foreign anorthosite.

Tonalite had very high SiO_2, Al_2O_3, and Na_2O contents, and far lower TiO_2, Fe_2O_3*, MnO, MgO and K_2O contents than those of the foreign tonalite (Arth et al., 1978). It may be because the tonalite had a very low mafic content, and because it was consisted mainly of quartz and plagioclase. This coincided with the AnRs, which has been explained previously.

The AfGr had relatively higher K_2O content and lower MgO and MnO contents than the other granites which will be explained later, and this was due to the concentration of K-feldspar, and to the low content of the mafic mineral.

K_2O/CaO ratio was maintained constantly from the AnRs to the tonalite, but was increased from the tonalite to the AfGr (Table 2). In comparing it with the average K_2O/CaO ratio of general plutonic rocks (Putmann and Burnham, 1963), the AnRs and the tonalite belonged to diorite/gabbro (<0.33), and the AfGr belonged to granite (>3.0). As in previous explanations, it indicated that the AnRs distributed in the studied area which were thought to have created the tonalite, or the tonalite and the AfGr in the late stage of differentiation, were differentiated under the potassium free condition during the stage when the AnRs and the tonalite were crystallized.

In comparing the D.I. of the Precambrian plutons with the Daly's value (Daly, 1914) of the average plutonic rocks, the AnRs belonged to gabbro (30)~diorite (48), the tonalite belonged to diorite~granodiorite (67), and the AfGr belonged to granite(80)~alkali granite (93).

The tonalite and the AfGr were plotted in the fields of tonalite, trondjhemite, and granite

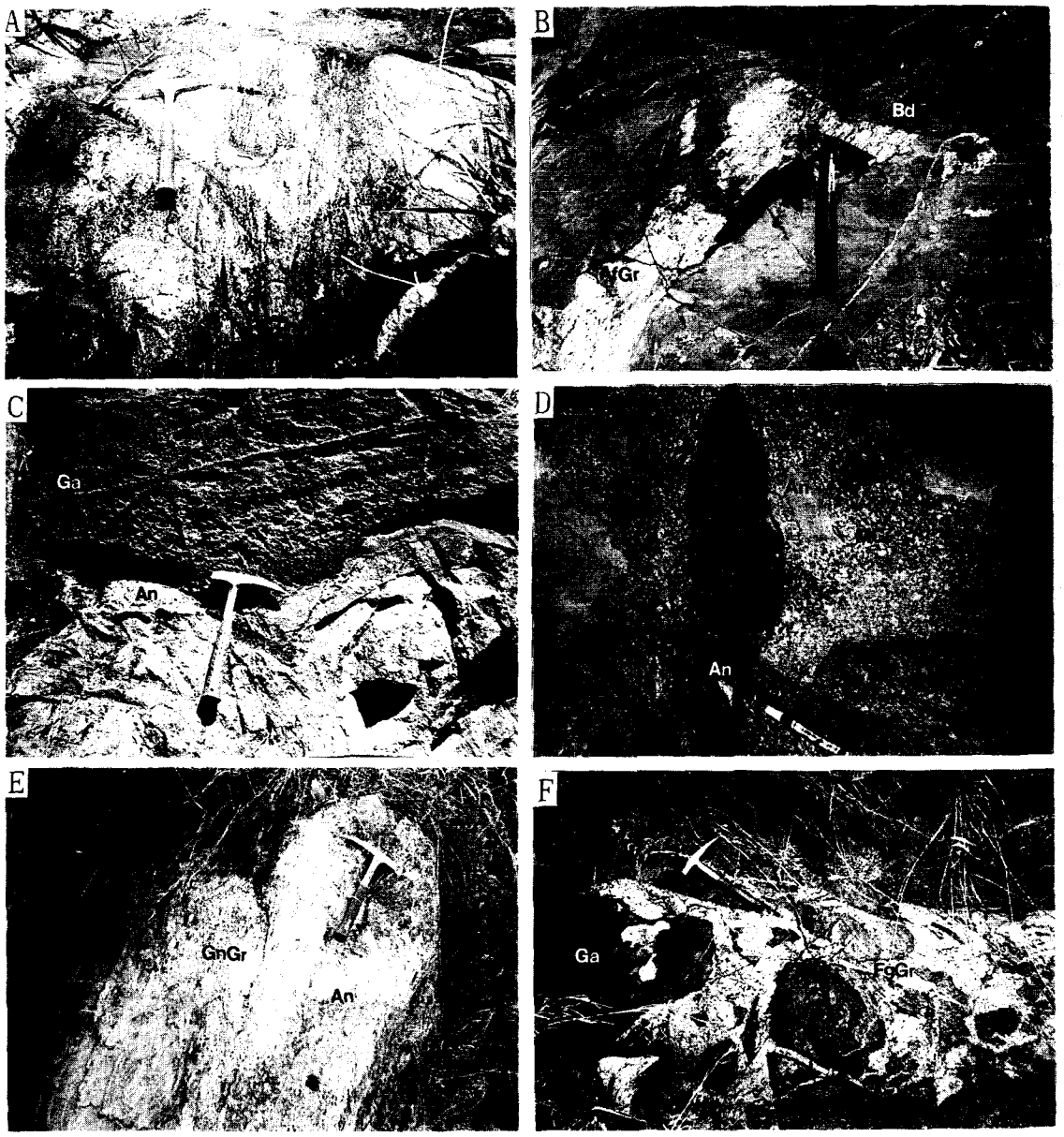

Fig. 3. Photographs of outcrops of the plutonic rocks. A: migmatitic gneiss; B: Alkali-feldspar granite (AfGr) which was intruded by the basic dyke (Bd); C: Foliation in anorthosite (An) which was cut by the gabbro (Ga); D: Xenolith of the anorthosite and the basic dyke in megacrystic granite (MGr); E: Xenolith of the gabbro in gneissose granite (GnGr); F: Xenolith of the gabbro in fine-grained granite (FgGr).

respectively in the triangular diagram of normative An-Ab-Or (Fig. 5). In the triangular diagram of Rb-Sr-Ba (Fig. 5), the tonalite was plotted in the field of diorite, and the AfGr was plotted in the fields of very differentiated granite, anomalous granite, and granodiorite dispersedly.

The trace elements, such as Ba, Y, and Zr, were increased from the AnRs through the tonalite to the AfGr (Fig. 6). Sr showed the trend that the concentration of the element was maintained constantly from the AnRs and the tonalite, but the trend from the tonalite to the AfGr was becreased. But they did not have continuity, and all of the major and trace elements had compositional gaps between each body.

In the diagram of the chondrite-normalized values to the atomic number of REEs (Rare Earth Elements) (Fig. 7), the AnRs showed a

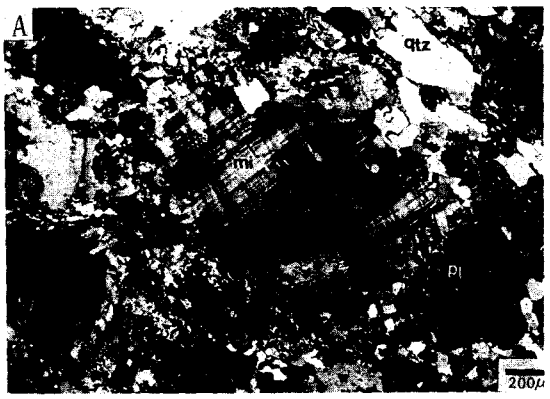

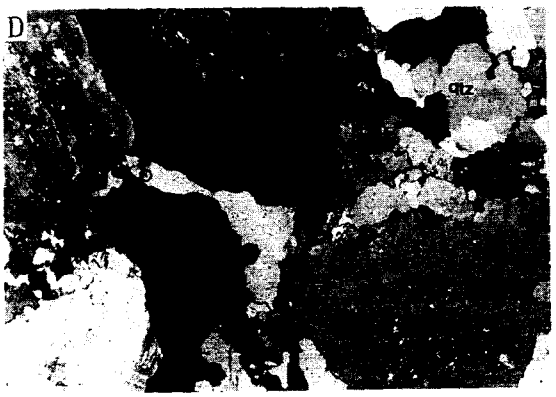

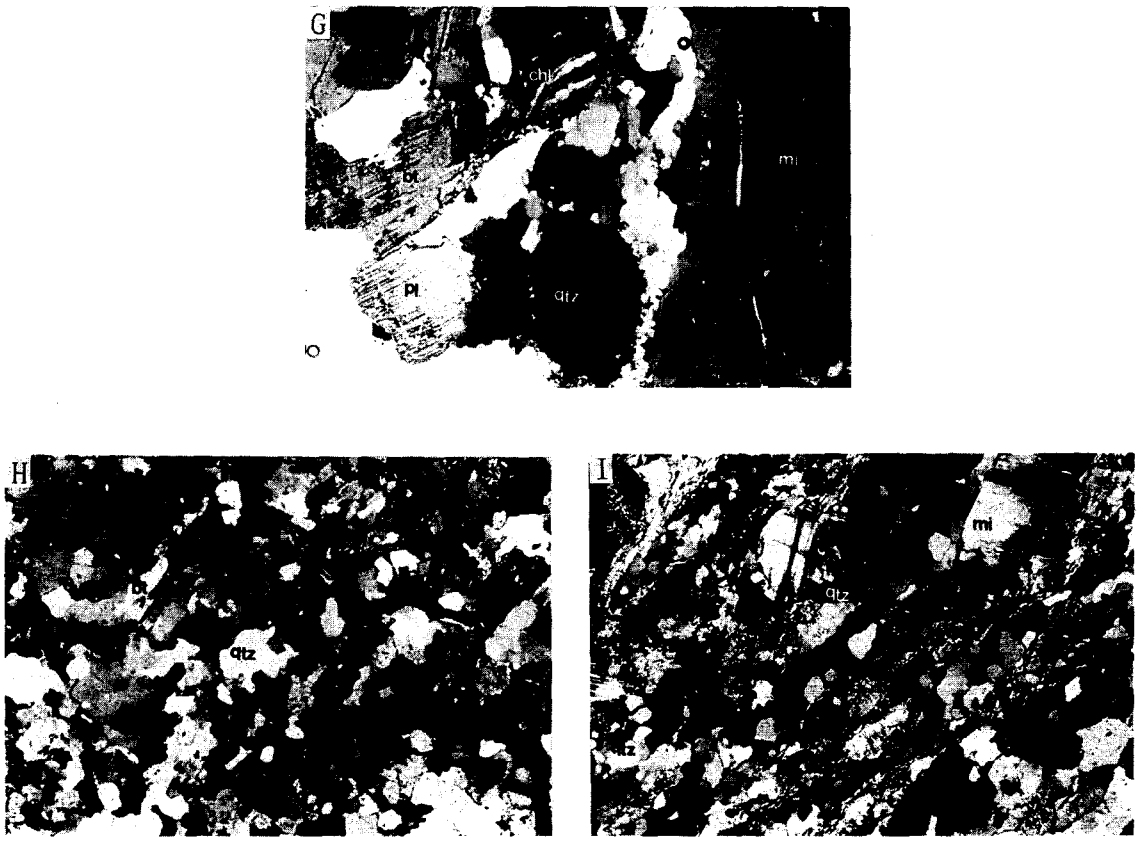

Fig. 4. Photomicrographs of the plutonic rocks in thin section. A: Microcline in migmatitic gneiss; Its edge shows partly melted trace. B: Anorthosite; Hornblende was crystallized among plagioclase cumulates. C: It is mainly composed of plagioclase and quartz. D: Alkali- feldspar granite; It is mainly composed of quartz and microcline. E: Basic dyke rock; It shows some hornblende phenocrysts. F: Gabbro; It shows subhedral plagioclase and reaction rim texture that hornblende replaced the edge of pyroxene. G: Megacrystic granite; It shows microcline megacrysts, and the mafic minerals are biotite. H: Fine-grained granite; It is mainly composed of fine-grained quartz, microcline and biotite. I: Gneissose granite; It shows gneissosity which has arrangement of biotites in one direction. qtz: quartz; mi: microcline; pl: plagioclase; hb: hornblende; px: pyroxene; chl: chlorite; bt: biotite. The scales are the same as in photo A.

strong positive Eu anomaly, and a somewhat unevolved pattern of 1 to 10 times of totally chondrite. Except for the strong positive Eu anomaly, the range of $(La/Lu)_N$ was low and narrow (3.91~6.52). The strong positive Eu anomaly is the particular pattern of anorthosite, and it is caused by the fractionation of plagioclase (Demaiffe, 1978).

Tonalite was wholly evolved five to twenty times as much as chondrite. Except for the Eu anomaly, it was wholly evenly distributed ($(La/lu)_N$=2.93~3.16). But the positive Eu anomaly of the tonalite was less strong than that of the AnRs. This means that the tonalite might be the product of the fractionation of the AnRs. and that the magmatic processes of the AnRs and the tonalite which had gradational relationships were controlled mainly by fractional crystallization.

The AfGr was wholly evolved three to fifty times as much as chondrite. LREEs were very depleted ($(La/Lu)_N$=0.24~0.49), and Eu showed a very strong negative anomaly in contrast with the AnRs and the tonalite. Demaiffe (1978) insisted that the residual liquid which remained after crystallization of plagioclase has a strong negative Eu anomaly. This means that the AfGr could be a product of the fractionation of the AnRs.

Table 2. Major element analyses and CIPW norms for the Precambrian plutonic rocks from Saengcho area (wt. %)

	Anorthositic rock						Tonalite			Alkali-feldspar granite		
	6-4	5-10	B-29	AP29-5	Feb14-1	Feb17-7	AP29-2	SP7-1	Ap29-6	WR	24-2	5-1-1
SiO_2	51.75	51.11	51.63	52.17	54.08	53.85	64.59	62.27	61.33	72.24	76.30	76.25
Al_2O_3	30.58	28.53	28.24	29.47	29.08	29.50	21.11	21.58	24.53	16.30	13.24	13.03
Fe_2O_3	0.57	2.12	1.90	0.63	0.44	0.31	0.85	0.44	0.54	0.36	0.61	0.75
CaO	13.10	12.53	12.80	11.64	11.43	11.42	4.59	6.10	7.49	3.14	0.90	0.64
MgO	0.25	1.60	1.48	0.25	0.16	0.09	0.41	0.12	0.14	0.07	0.43	0.03
Na_2O	3.73	3.50	3.43	4.67	4.28	4.72	4.43	5.70	5.41	5.68	3.45	3.64
K_2O	0.26	0.50	0.28	0.20	0.42	0.32	1.94	0.48	0.62	1.98	5.02	5.54
TiO_2	0.08	0.13	0.19	0.10	0.09	0.09	0.11	0.04	0.09	0.02	0.04	0.04
MnO	0.01	0.03	0.03	<0.01	0.01	<0.01	0.01	<0.01	0.01	<0.01	0.07	0.11
P_2O_5	<0.02	<0.02	<0.02	<0.02	<0.02	<0.02	<0.02	<0.02	<0.02	<0.02	<0.02	<0.02
LOI	0.55	0.83	0.65	0.88	0.78	0.66	1.48	0.80	0.77	0.96	0.64	0.30
Total	100.81	100.81	100.60	100.04	100.79	100.99	99.54	97.56	100.95	100.78	100.72	100.35
K_2O/CaO	0.02	0.04	0.02	0.02	0.04	0.03	0.42	0.08	0.08	0.63	5.58	8.66
q	0.37	-	0.51	-	2.69	0.49	20.56	13.84	11.01	25.13	34.10	32.03
or	1.54	2.95	1.65	1.18	2.48	1.89	11.46	2.84	3.66	11.70	29.66	32.74
ab	31.56	30.04	29.02	38.53	36.21	39.94	37.48	48.23	45.77	48.06	29.19	30.80
an	64.86	60.43	60.83	57.61	56.57	56.52	22.64	30.13	37.03	13.13	4.33	2.85
ap	<0.05	<0.05	<0.05	<0.05	<0.05	<0.05	<0.05	<0.05	<0.05	<0.05	<0.05	<0.05
il	0.15	0.25	0.36	0.19	0.17	0.17	0.21	0.08	0.17	0.04	0.08	0.08
c	0.39	-	-	0.46	0.85	0.67	3.43	0.64	1.39	-	0.54	-
mt	0.10	0.37	0.33	0.11	0.08	0.05	0.15	0.08	0.09	0.06	0.11	0.13
di di	-	0.81	1.33	-	-	-	-	-	-	0.38	-	0.01
di hd	-	0.49	0.74	-	-	-	-	-	-	0.90	-	0.16
hy en	0.62	0.25	3.07	-	0.40	0.22	1.02	0.30	0.35	0.23	1.07	0.07
hy fs	0.67	0.17	1.95	-	0.47	0.29	1.00	0.56	0.61	0.64	0.90	1.08
ol fo	-	2.35	-	0.44	-	-	-	-	-	-	-	-
ol fa	-	1.79	-	0.55	-	-	-	-	-	-	-	-
ne	-	-	-	0.53	-	-	-	-	-	-	-	-
salic	98.72	93.42	92.01	98.31	98.80	99.51	95.57	95.68	98.86	98.02	97.82	98.42
femic	1.59	6.53	7.84	1.87	1.17	0.78	2.43	1.07	1.27	2.30	2.21	1.58
D. I.	33.47	32.99	31.18	40.25	41.38	42.32	65.50	64.90	60.44	84.89	92.25	95.57

Table 3. Trace element analyses for the Precambrian plutonic rocks from Saengcho area (ppm)

	Anorthositic rock						Tonalite			Alkali-feldspar granite			Gneiss
	6-4	5-10	B-29	AP29-5	Feb14-1	Feb17-7	AP29-2	SP7-1	Ap29-6	WR	24-2	5-1-1	Average
Rb	<10	<10	<10	<10	25	18	85	10	21	53	120	160	
Sr	393	330	332	405	389	410	358	369	333	200	115	21	114.5
Ba	55	68	59	49	56	86	87	103	75	313	351	52	963.5
Sc	0.4	4.9	5.3	0.6	0.3	0.2	1.0	0.5	2.2	0.5	1.6	1.2	
Y	1	2	3	4	4	3	20	20	11	16	53	103	
La	1.3	1.9	1.4	1.9	1.3	2.1	5.4	4.3	5.1	3.4	4.0	3.3	59.5
Ce	3	3	<3	4	<3	3	12	9	11	13	14	16	108.8
Nd	<5	<5	<5	<5	<5	<5	16	<5	6	7	10	11	49.7
Sm	0.2	0.3	0.2	0.3	0.2	0.3	1.4	1.2	1.1	2.6	3.9	5.1	9.6
Eu	0.7	0.8	0.7	0.6	0.7	0.6	0.9	0.6	0.7	0.3	0.2	<0.2	1.3
Tb	0.5	0.5	0.5	<0.5	<0.5	<0.5	0.5	0.5	<0.5	1.0	1.2	2.0	
Yb	<0.2	0.2	0.2	0.27	<0.2	0.2	1.15	1.22	1.1	7.6	5.8	10.1	5.3
Lu	<0.01	0.03	0.03	0.05	<0.01	0.04	1.19	0.14	0.17	0.94	0.83	1.41	0.8
Th	<0.5	<0.5	<0.5	<0.5	<0.5	<0.5	4.9	10	3.6	6.6	6.6	8.3	
Zr	<1	<1	<1	4	10	13	80	48	33	157	126	130	
V	10	28	26	<2	6	8	8	<2	8	<2	46	4	

Table 4. Major element analyses and CIPW norms for the Jurassic plutonic rocks from Saengcho area (wt. %)

	Gabbro					Megacrystic granite			Fine-grained granite		Gneissose granite		
	G1	G2	G3	OB27-6	Feb16-5	AP29-10	OB28-5	OB29-11	OB29-8	OB29-10	Mal-1	AP26-2	De12-4
SiO_2	51.29	44.80	46.18	51.12	47.79	61.06	67.70	65.75	74.17	73.74	70.88	75.28	76.71
Al_2O_3	18.39	16.10	15.35	18.08	13.23	19.04	15.63	16.10	13.75	14.61	13.81	14.15	12.48
Fe_2O_3	9.13	12.02	10.36	9.56	17.19	3.64	4.01	3.97	1.53	1.31	2.63	0.68	0.78
CaO	9.15	12.83	18.08	8.99	9.78	5.41	2.67	2.96	1.20	0.81	0.82	1.02	0.98
MgO	5.01	8.10	7.18	5.81	5.70	0.92	0.81	0.94	0.28	0.16	0.46	0.11	0.06
Na_2O	3.59	2.02	1.21	3.25	2.43	4.35	3.77	4.09	3.82	4.95	2.63	3.65	2.23
K_2O	1.02	0.36	0.14	0.56	0.52	2.84	4.70	3.80	4.88	3.98	5.47	5.10	6.42
TiO_2	1.19	1.03	0.77	0.86	3.24	0.38	0.55	0.49	0.24	0.13	0.33	0.08	0.07
MnO	0.15	0.18	0.19	0.16	0.23	0.06	0.07	0.08	0.06	0.03	0.03	0.02	0.01
P_2O_5	0.14	0.12	0.28	0.32	0.20	0.10	0.18	0.18	0.04	0.02	0.06	<0.02	<0.02
LOI	0.96	0.40	0.33	0.83	0.01	0.82	0.43	0.71	0.52	0.49	0.80	0.78	0.31
Total	100.02	97.96	100.07	99.54	100.32	99.62	100.52	99.07	100.49	100.23	97.92	100.89	100.07
K_2O/CaO	0.11	0.03	0.01	0.06	0.05	0.52	1.76	1.28	4.07	4.91	6.67	5.00	6.55
q	-	-	-	-	-	10.56	19.27	18.01	29.58	27.06	30.96	31.86	36.60
or	6.03	2.13	0.83	3.31	3.07	16.78	27.77	22.45	28.84	23.52	32.32	30.14	37.94
ab	30.38	13.13	5.61	27.50	20.56	36.81	31.90	34.61	32.32	41.88	22.25	30.88	18.87
an	31.05	33.80	36.04	33.09	23.66	24.04	11.84	13.51	5.69	3.89	3.68	4.93	4.73
ap	0.33	0.28	0.66	0.76	0.47	0.24	0.43	0.43	0.09	0.05	0.14	0.05	0.05
il	2.26	1.96	1.46	1.63	6.15	0.53	1.04	0.93	0.46	0.25	0.63	0.15	0.13
c	-	-	-	-	-	-	-	0.31	0.10	0.73	2.22	0.82	0.13
mt	1.59	2.09	1.80	1.66	2.99	0.63	0.70	0.69	0.27	0.23	0.46	0.12	0.14
di di	7.13	14.41	25.78	4.50	9.17	0.66	0.06	-	-	-	-	-	-
hd	5.39	9.41	16.68	3.24	10.49	1.16	0.13	-	-	-	-	-	-
hy en	3.97	-	-	11.64	8.92	1.99	1.99	2.34	0.70	0.40	1.15	0.27	0.15
fs	3.44	-	-	9.63	11.70	4.02	4.65	4.78	1.81	1.64	3.11	0.84	0.97
ol fo	3.65	9.45	4.16	0.52	0.72	-	-	-	-	-	-	-	-
fa	3.48	7.80	3.40	0.48	1.04	-	-	-	-	-	-	-	-
ne	-	2.14	2.51	-	-	-	-	-	-	-	-	-	-
salic	67.46	51.20	44.99	63.90	47.29	88.19	90.78	88.89	96.53	97.08	91.43	98.63	98.27
femic	31.24	45.40	53.94	34.06	51.65	9.23	8.99	9.17	3.33	2.57	5.49	1.43	1.44
D. I.	36.40	17.40	8.95	30.81	23.63	64.15	78.94	75.07	90.74	92.46	85.54	92.88	93.41

Table 5. Trace element analyses for the Jurassic plutonic rocks from Saengcho area (ppm)

	Gabbro					Megacrystic granite			Fine-grained granite		Gneissose granite		
	G1	G2	G3	OB27-6	Feb16-5	AP29-10	OB28-5	OB29-11	OB29-8	OB29-10	Mal-1	Ap26-2	De12-4
Rb	41	<10	<10	<10	<10	54	100	88	73	75	280	85	140
Sr	478	338	475	493	267	354	223	263	126	192	129	179	81
Ba	441	148	102	282	170	1091	1539	1405	1116	1105	873	962	280
Sc	31	35	22	21	34	8.1	8.6	12	2.8	0.7	4.1	0.9	0.6
Y	40	26	12	19	37	24	37	37	17	11	18	6	4
La	16.6	9.3	5.1	8	14.6	47.1	65.4	69.4	14.5	12.6	67.7	6.1	4.9
Ce	40	26	13	16	29	88	115	136	29	24	134	18	12
Nd	24	14	7	9	22	33	50	50	11	9	49	8	5
Sm	6	4.1	2.3	2.6	5.1	5.9	7.5	7.8	1.9	1.5	6.8	0.6	0.9
Eu	1.4	0.9	0.8	1.0	1.6	1.4	1.4	1.4	0.5	0.5	0.9	0.4	0.5
Tb	0.9	<0.5	<0.5	0.5	1.2	0.6	1.0	1.2	<0.5	<0.5	<0.5	<0.5	<0.5
Yb	2.95	2.37	1.04	1.5	3.0	1.45	2.5	3.2	1.4	1.4	1.58	0.6	0.4
Lu	0.46	0.35	0.18	0.21	0.44	0.26	0.40	0.5	0.22	0.23	0.29	0.11	0.08
Th	1.8	<0.5	<0.5	<0.5	0.6	9.9	13	16	9.0	2.7	47	2.9	13
Zr	91	55	46	49	188	289	314	340	171	158	272	82	81
Hf	1.9	1.2	1.1	0.5	3.9	5.3	8.1	7.7	3.4	3.3	8.0	1.9	2.1
Co	23	43	35	24	49	5	4	4	2	<1	8	2	1

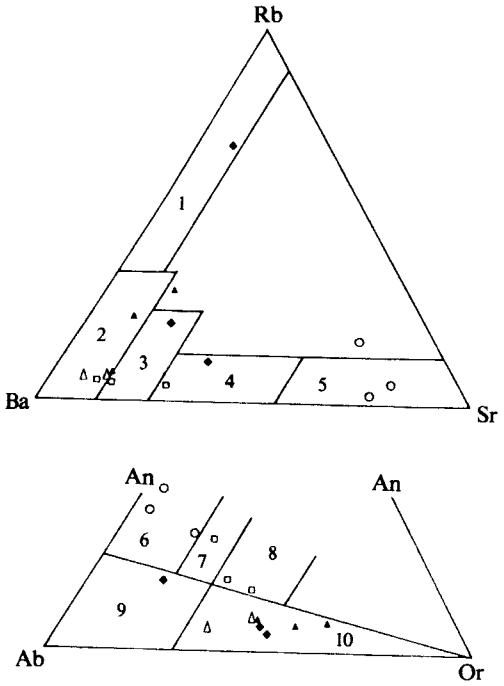

Fig. 5. Ternary plots of Rb-Ba-Sr and An-Ab-Or for the granitic rocks. Symbols are the same as in Fig. 2. Diagram is from El Bouseily and El Sokkary (1975) and O'connor (1965). 1: Very differentiated granite; 2: Normal granite; 3: Anomalous ganite; 4: Granodiorite; 5: Diorite; 6: Tonalite; 7: Granodiorite; 8: Adamelite; 9: Trondjhemite; 10: Granite

Jurassic Plutonic Rocks

These plutons showed linear trends in the variation diagram of the major and the trace elements to D.I. (Fig. 8) seemingly that they were differentiated from a same magma. But K_2O and Na_2O showed a somewhat dispersed tendency. D.I. showed a very broad variation in each body (gabbros: 8.95~36.4, granites: 64.15~93.4). This may indicate that the crystallization of their original magma was controlled by fractional crystallization. But there was somewhat of a composition al gap between the gabbro and the MGr. This in dicated that these rocks were differentiated from the other magmas in their origin, or that the rocks which had the intermediate chemical composition of each rock did not occur on the surface.

In comparing the D.I. of the Jurrasic plutons

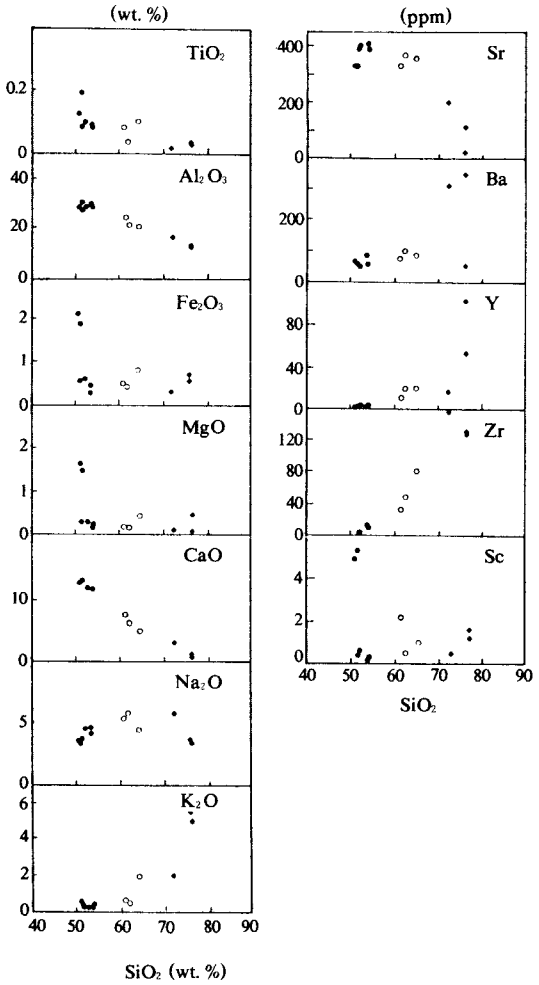

Fig. 6. Variation diagrams of oxides and trace elements to silica for the Precambrian plutonic rocks. symbols are the same as in Fig. 2.

with Daly's value (Daly, 1914) of average plutonic rocks, the gabbro belonged to peridotite (6)~gabbro (30), the MGr belonged to granodiorite (67)~granite (80), the GnGr belonged to alkali-granite (93), and the FgGr belonged to Granite~alkali-granite.

K_2O/CaO ratio was gradually increased from the gabbro to GnGr (Table 4). Compared with the average K_2O/CaO ratio of general plutonic rocks, the gabbro belonged to diorite/gabbro (<0.33), the MGr belonged to granodiorite (1.5~0.60) or quartz monzonite (3.0~1.5), and the FgGr and the GnGr belonged to granite.

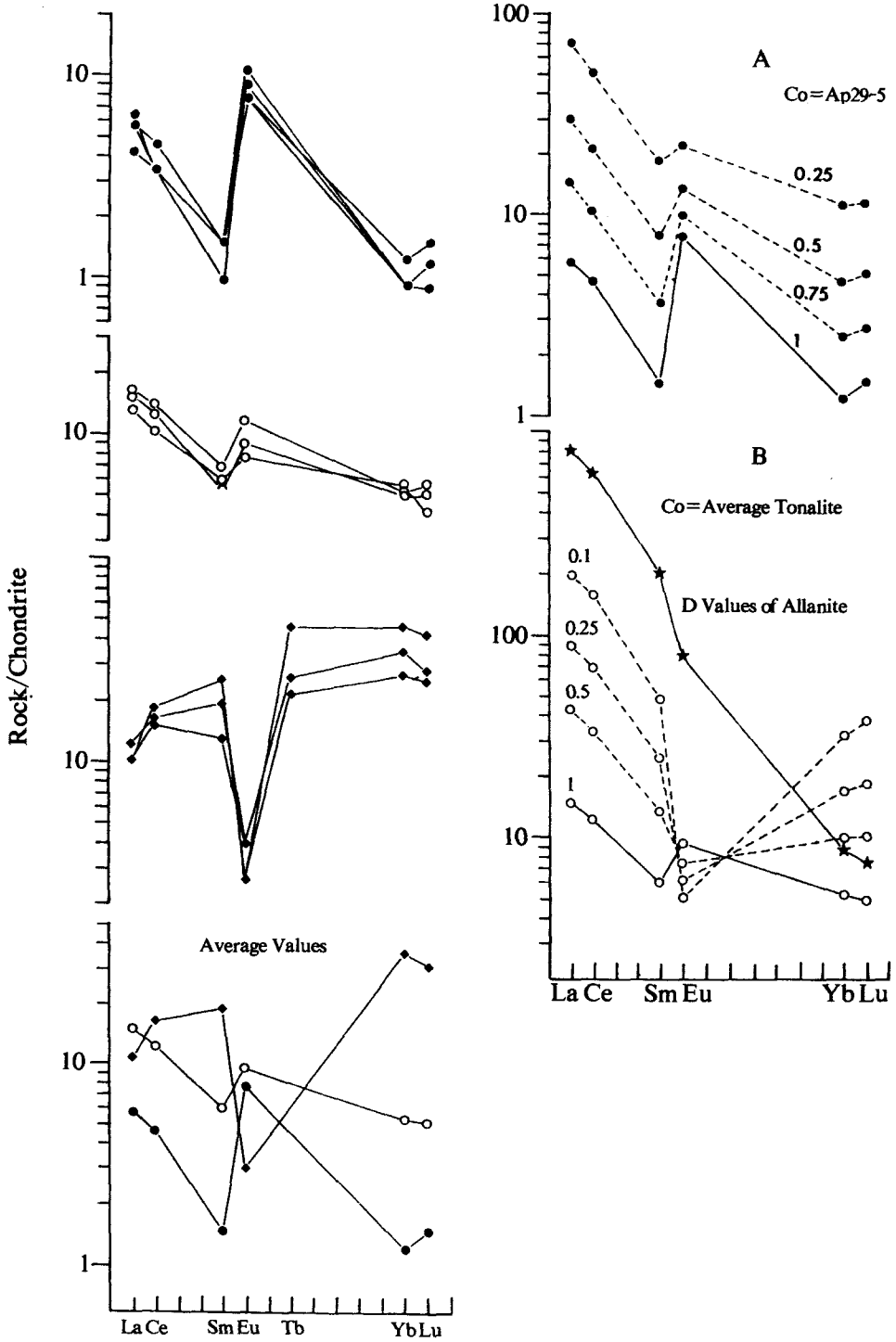

Fig. 7. Chondrite-normalized REE patterns and AFC models (r=0.1) for the Precambrian plutonic rocks. D values of allanite are from Henderson (1984). Normalizing factors are from Nakamura (1974). Symbols are the same as in Fig. 2.

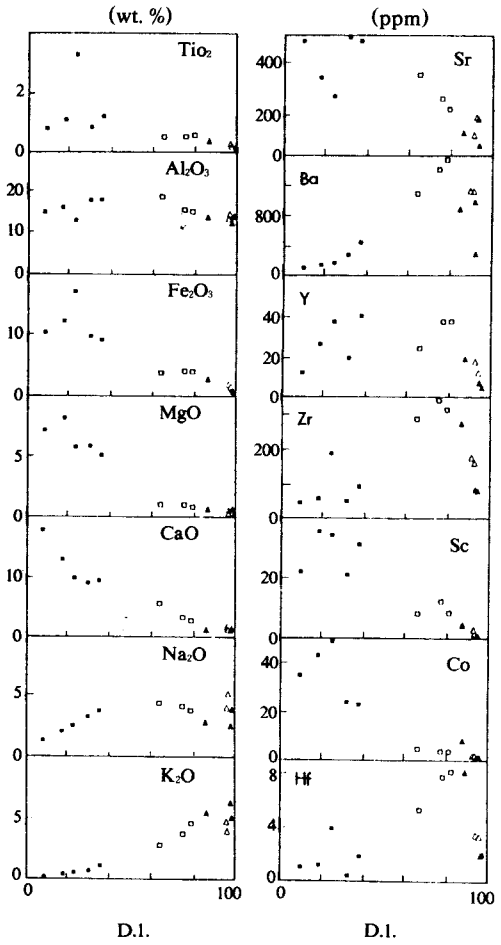

Fig. 8. Variation diagrams of oxides and trace elements to D. I. for the Jurassic plutonic rocks. Symbols are the same as in Fig. 2.

The MGr was plotted in the fields of granodiorite and adamelite, and the FgGr and GnGr were plotted in the field of granite in the triangular diargam of normative An−Ab−Or (Fig. 5). All rocks were plotted near the boundary between normal granite and anomalous granite in the triangular diagram of Rb−Ba−Sr (Fig. 5).

The concentration of the elements, such as Sr, Sc and Co, decreased gradually from the gabbro to the GnGr (Table 5). Y was maintained constantly from the gabbro to the MGr, but it decreased rapidly from the MGr to the GnGr. These phenomena may have occurred because Sc and Co are compatible with mafic minerals such as pyroxene, hornblende and biotite, because Sr is compatible with plagioclase and K−feldspar, and because Y is compatible with hornblende and with some accessary minerals. They corresponded with the variation of the modal composition of the Jurassic plutonic rocks. The elements such as Zr, Hf and Ba showed a tendency for their concentration to increase rapidly from the gabbro and the MGr, but to decrease from the MGr to GnGr. This also corresponded with the variation of the modal composition of some accessary minerals including hornblende, biotite, and K-feldspar with which these elements are compatible.

The gabbro was evolved 7~25 times as much as chondrite (Fig. 9), and showed the pattern that all REEs were distributed evenly ($(La/Lu)_N$=2.73 ~3.29). The patterns which ranged from the very weak positive Eu anomaly to the negative Eu anomaly were shown, and this means that the fractional crystallization acted during the differentiation of the magma.

The MGr was evolved 7~200 times as much as chondrite, and showed the pattern that LREEs were very enriched and the HREEs had a gentle slope. It showed a very weak negative Eu anomaly to the negative Eu anomaly. It was also because the fractional crystallization acted during the differentiation of the magma.

The FgGr was evolved 6~40 times as much as chondrite. Since LREEs were very enriched, it had very similar pattern to the MGr, but all REEs were depleted more than that of the MGr.

The GnGr was evolved 2~200 times as much as chondrite. It showed two different patterns: one type was similar to the MGr, and the other type had a positive Eu anomaly, and were wholly very depleted (2~20 times of chondrite). The former had a very similar pattern to the MGr (Ma 1−1), and showed gneissosity, but had a similar mineral composition to the MGr. It might be inferred to be the product of the intermediate step between the MGr and the GnGr.

TRACE ELEMENT MODELLING

It was expected that the rocks which had comagmatic relationships among one another would be located. So, to clarify this, and to expli-

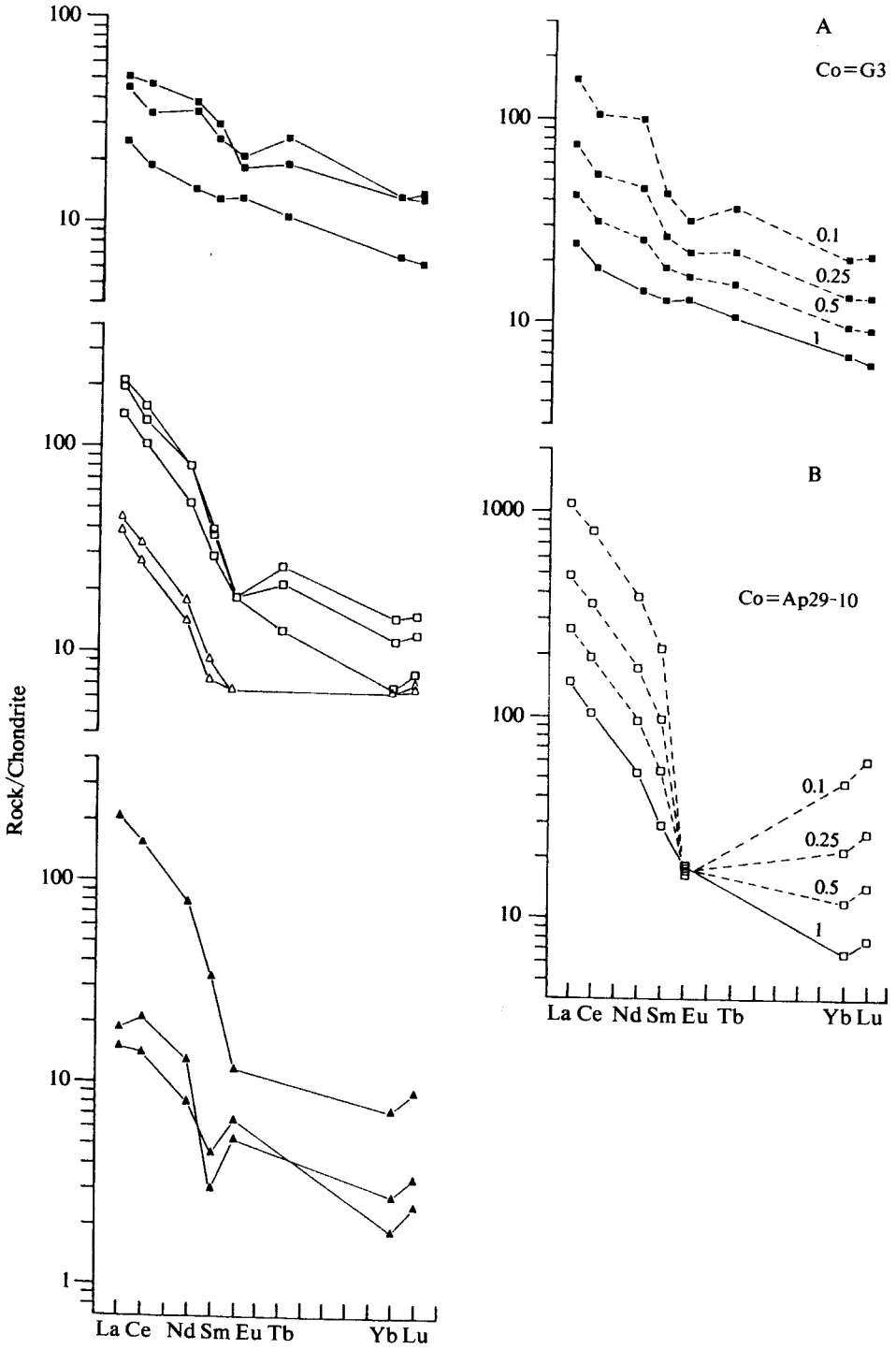

Fig. 9. Chondrite-normalized REE patterns and RCF models for the Jurrassic plutonic rocks. D values of the accessary minerals are from Henderson (1984). Normalizing factors are from Nakamura (1974). Symbols are the same as in Fig. 2.

cate the process of magmatic differentiation, the models for the magmatic differentiation were calculated.

Jeong (1987) reported that the chemical composition of the magma which created the AnRs varied during the differentiation by the wall–rock assimilation. Kwon and Jeong (1990) found that the anorthositic magma originated from the mantle, but that it would be assimilated with crustal material. Therefore, it might be most reasonable to use the AFC (Assimilation and Fractional Crystallization) model (Depaolo, 1981) to study the Precambrian plutonic rocks. It is the best model for fractional crystallization which accompanied wall–rock assimilation.

Rayleigh's Crystal Fractionation Law was applied to the study of the Jurassic plutonic rocks, because they had obvious contact with each other, and because some geochemical characteristics explained previously indicated that the fractional crystallization acted in the differentiation of the magma. It is generally thought to be an ideal model for the fractional crystallization in the closed system.

Hong (1990) suggested that several attempts at a petrogenetic study of the intrusive rock systems have been used on the LIL elements: Rb, Sr and Ba, and that these elements are particularly useful for trace element modelling purposes in the granitic system, since they occur only in the major silicate minerals, but not in the accessary components. For the same reason, the elements that were suggested above may be very useful for trace element modelling purposes, not only in the granitic system, but also in a complex system such as the Jurassic plutons in this area. REEs are the important index in the study of the magmatic process, since the radius of the ions increases gradually (Mason et al., 1982). Thus, Sr, Ba, and REEs were used for the trace element modelling in this study.

The distribution coefficients of Sr and Ba, which were used in the model calculation, were quoted from Arth et al.(1981) for the Precambrian plutons and from Cox et al.(1979) for the Jurassic plutons. The distribution coefficients of REEs were quoted from Henderson (1982).

Precambrian Plutonic Rocks

The rock assumed as a contaminent in the AFC model (Fig. 10) was the granitic gneiss, bordering the southern part of the AnRs. The average value of 7 specimens was used (Table 3). The sample which was selected as Co (Concentration of Original melt) was AP29–5. It was inferred to have crystallized at the earliest stage in the relationship of Sr and Ba. It was assumed that the 95% of plagioclase and 5% of hornblende were crystallized during the whole stage.

The trend of evolution from the AnRs, through the most typical tonalite to the most typical AfGr, lies near to the fractionation curve of AFC [r(assimilation rate/crystallization rate)=0.1]. It means that the assimilation proceeded at the speed of 0.1 times of crystallization.

Based on the result ($r \leq 1$) of above model, the model for REEs was calculated(Fig. 7A and 7B). The tonalite had a very similar pattern to that of the model (F=0.5) (Fig. 7A). But D value of REEs varied sensitively according to the variation of the composition of the melt. Thus, the model for the tonalite was calculated again (Fig. 7B). In the recalculated model, the AfGr had a very similar Eu anomaly to the modeol (F=0.1), but it showed a pattern where LREEs were relatively depleted

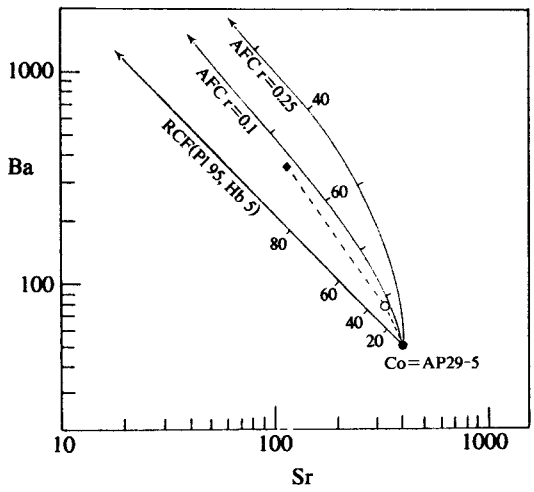

Fig. 10. Trace elements relationship and AFC model for the Precambrian plutonic rocks. Symbols are the same as in Fig. 2.

(Fig. 7B). It could not be explained by the simple fractionation of major minerals. The phases which are very compatible with LREEs, such as allanite (Fig. 7B), had to fractionate before the crystallization of the AfGr, to explain the depletion of LREEs. Taking account of the confirmed epidote in the modal composition of the anorthositic rocks and the tonalite, its validity can be recognized (Table 1).

Jurassic Plutonic Rocks

Assuming a crystallization of 2.6% of orthopyroxene, 7.8% of clinopyroxene, 37.7% of hornblende, 6.3% of biotite, and 45% of plagioclase, the fractionation curve of the gabbro passed close to the MGr in the Rayleigh's fractionation model of Ba to Sr (Fig. 11). This means that these rocks could be related originally, and if this was true, it means that the differentiation of the gabbro was controlled by the above mineral assemblage. Because the gabbro had to be fractionated more than 90% to create the MGr in the result of the model, and because the distributed area of the granits was wider than that of the gabbro

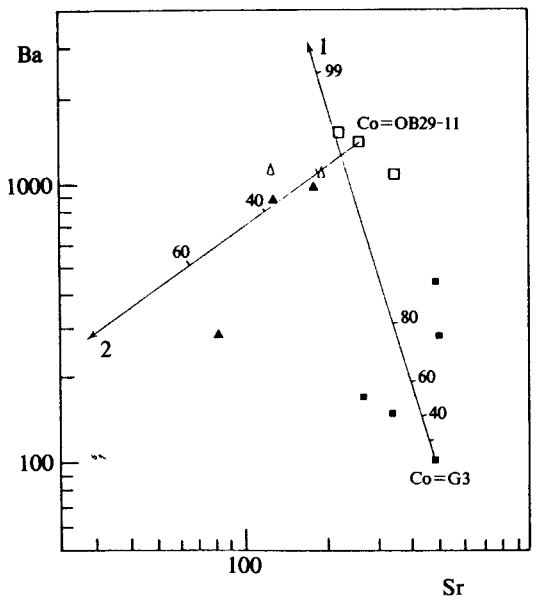

Fig. 11. Trace elements relationshp and RCF model for the Jurassic plutonic rocks. Symbols are the same as in Fig. 2. 1: Co=Gabbro; 2: Co=Megacrystic granite.

(Kim et al., 1964), it was somewhat difficult to accept that those rocks were products of the simple fractionation of the single gabbroic magma. The model from which the MGr was selected as Co assumed that the average mineral composition of the MGr (35% of quartz, 1.5% of hornblende, 5% of biotite, 35% of plagioclase, 25% of K−feldspar) were fractionated (Fig. 11). The fractionation curve corresponded with the composition of the FgGr and of the GnGr. This means that the differentiation of the MGr, the FgGr and the GnGr was controlled by the fractionation of the above mineral assemblage.

In the fractionation model for REEs (Fig. 9A), the negative Eu anomaly was increased, and Nd was enriched from F=1 to F=0.1. By this model, that the above mineral assemblage was fractionated, MGr could not be created, and it means that the gabbro and the MGr at least were not crystallized by simple fractionation in a same magma chamber. Considering that the MGr intruded gabbro, and that the intermediate rocks of these two rocks did not exist, it could be estimated that the gabbro and the granites were not the products of the simple fractionation of the same magma.

In the fractionation model in which the MGr was selected as Co (Fig. 9B), all REEs, except for Eu, were enriched. It was relatively consistent with other MGr, but it was not consistent with the FgGr and the GnGr, which had gradational relationships with the MGr. They showed a very depleted pattern rather than the enriched pattern. It could hardly be explained by the simple crystal fractionation of the above mineral assemblage. Therefore, the other factors which acted on the crystallization were nessassary to explain the differentiation process.

REEs are very compatible with the accessary minerals such as allanite, zircon and sphene, rather than the major minerals (Fig. 12). The uncommon REEs distribution pattern could result mainly from the fractionation of particular mineral such as hornblende, and some accessary minerals during magmatic evolution, since hornblende had an especially high distribution coefficient for all REEs in the silicic magma (Henderson, 1984). About 50% of hornblende and about

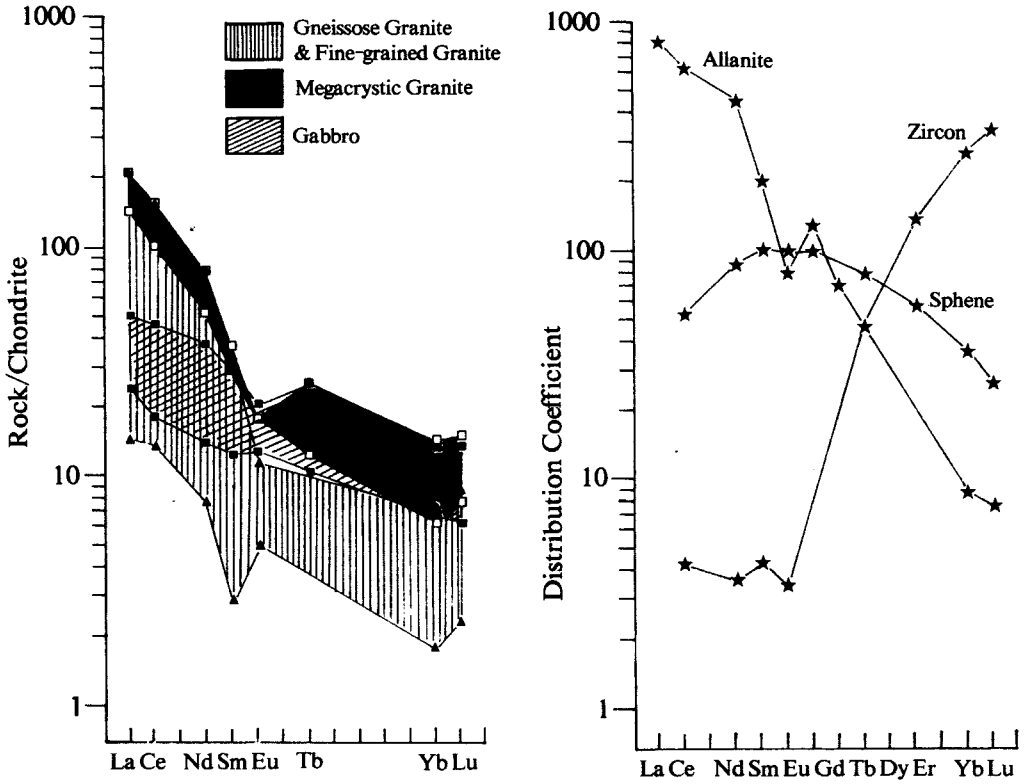

Fig. 12. Chondrite-normalized REE abundances in the Jurassic plutonic rocks and Distribution coefficients of some accessary minerals. D values of the accessary mineals are from Henderson (1984). Normalizing factors are from Nakamura (1974). Symbols are the same as in Fig. 2.

0.5% of accessary minerals must be fractionated to make the pattern that all the REEs were depleted, like those granites. But about 9% of hornblende and about 0.5% of accessary minerals, in maximum, were contained in the MGr. This means that the depletion of REEs might be due not only to the fractionation of those minerals, but also to other factors.

DISCUSSION

Anorthosite and Related rocks

The anorthosites which were distributed in many other countries were composed of many kinds of related rocks (for example, from ultramafic rocks to acidic rocks) which were differentiated accompanied by anorthosite. Considering that the AnRs were derived from mantle (Kwon and Jeong, 1990), the parental magma of AnRs might not be composed of only anorthositic composition. Thus, the rocks which were differentiated accompanied by the AnRs may be inferred to exist. It could be suggested that Fe, Mg, Na and K were lacking in the AnRs, as evidence of this.

It was observed that the AnRs, among the rocks which occurred on the surface, were differen-tiated from the AnRs through the tonalite to AfGr in the results of this study. And, it was confirmed that the rocks which were mainly composed of quartz, biotite and plagioclase were distributed similarly with tonalite in the Sancheong district, which bordered the southern part of this area (Lee, 1991). Consequently, it was considered that it was formed by residual liquid after crystallization of AnRs, and K and Na were consumed as major compositions in the crystalli-

zation of the rock which crystallized after the formation of the AnRs. But the rocks which could supplement Fe, Mg to the rocks which were differentiated from gabbroic magma derived from mantle were not found. Thus, it was expected that the rocks which were differentiated before the crystallization of the AnRs may have continued under the surface. In fact, considering this in relation to the origin of anorthosite, its possibility cannot be excluded. Three other bodies which had similar origins with this were the Skaergaard Intrusion (Wager and Brown, 1967), the Mineral Lake Intrusion (Olmsted, 1968), and the Nain Anorthosite Series (Morse, 1968).

Assimilation

Jeong (1987), and Kwon and Jeong (1990) made clear that the magma which created the AnRs accompanied crustal assimilation during the intrusion. This means that the differentiation of the AnRs did not proceed under the closed system, and this was consistent with the result of the AFC model that the assimilation proceeded at the rate of $r \leq 0.1$. However, it does not mean that the result of the model can cover the whole body of AnRs, but it means that it can cover only the studied area. It was because the assimilation did not proceed at the same rate in all contacts with other rocks, and because the chemical composition of the wall−rocks was not homogeneous, when the magma had intruded. As an example of this, it can be suggested that the gneiss complex which the AnRs intruded was composed of many kinds of gneisses which had different chemical compositions and had different structures. And because the assimilation rate which was calculated by the AFC model means assimilation proceeded after the beginning of the fractional crystallization, the information about assimilation which proceeded before the beginning of the fractional crystallization cannot be estimated. Thus, further study about this will have to be undertaken, and it must not be neglected that the values ($r \leq 0.1$) cannot cover the whole body of AnRs.

CONCLUSION

The studied area was composed mainly of the anorthositic rocks and its related rocks, the basic dykes of unknown age, the Jurassic gabbro, and the granites of unknown age which intruded above the plutonic rocks. The related rocks of the anorthositic rocks were the tonalite and the alkali-feldspar granite, and the granites consisted of the megacrystic granite, the fine- rained granite, and the gneissose granite.

The anorthositic rocks distributed in the studied area were probably differentiated from the anorthositic rocks through the tonalite to the alkali-feldspar granite. This is to say, the tonalite and the alkali-feldspar granite are the products of the differentiation of the anorthositic rocks, and they were differentiated under the K, Mg and Fe lack/free condition.

According to the result of the AFC model, they were differentiated mainly by fractional crystallization, and the assimilation of wall-rocks proceeded at the rate of $r \leq 0.1$ during the differen-tiation.

The gabbro, the megacrystic granite, the fine-grained granite and the gneissose granite, which all intruded the anorthositic rocks subsequently, did not have any original relationships with the anorthositic rocks, and they were formed by repeated intrusion of magmas, which may or may not be the same in its origin. According to the result of the RCF model, these plutonic rocks were differentiated by simple fractional crystallization, and they assimilated relatively less than the anorthositic rocks.

Acknowledgments: This study was supported financially by the Korea Science and Engineering Foundation (1988. 9~1991. 8). We thank Dr. Kim, Seon-Eok of Korea Institute of Energy and Resources for all the assistance he rendered with chemical analysis, and Drs. Jin, Myung-Shik, Lee, Jin-Soo, and Hong, Young-Kook of Korea Institute of Energy and Resources for constructive criticism and advice during the preparation of this research.

REFERENCES

Arth, J.G., Barker, F., Peterman, Z.E. and Friedman, I. (1978) Geochemistry of the gabbro-diorite-tonalite-trondhjemite suite of Southwest Finland and its implications for the origin of tonalitic and trondhjemitic magmas. Journal of Petrology, 19, 289-316.

Cox, K.G., Bell, J.D. and Pankhurst, R.J. (1979) The Interpretation of Igneous Rocks. George Allen & Unwin Ltd.

Daly, R.A. (1914) Igneous Rocks and their Origin. New York, McGraw-Hill.

Demaiffe, D. and Duchesne, J.C. (1978) Trace elements and anorthosite genesis. Earth and Planetary Science Letters, 38, 249-272.

DePaolo, D.J. (1981) Trace element and isotopic effects of combined wall-rock assimilation and fractional crystallization. Earth and Planetary Science Letters, 53, 289-202.

El Bouseily, A.M. and El Sokkary, A.A. (1975) The relation between Rb, Ba and Sr in granitic rocks. Chem. Geol., 16, 207-220.

Green, T.H. (1968) Experimental fractional crystallization of quartz diorite and its application to the problem of anorthosite origin. Second Annual George H. Hudson Symposium 1966, 18, 23-29.

Henderson, P. (1984) Rare Earth Element Geochemistry. Elsvier Science Pul. 510.

Herz, N. (1968) The Roseland alkalic anorthosite massif, Virginia. Second Annual George H. Hudson Symposium 1966, 18, 357-368.

Hong, Y.K. (1990) Petrogenetic modelling of the vertically zoned cretaceous Pohang epizonal intrusive rocks, SE Korea. J. Geol. Soc. Korea, 27, 64-86.

Hwang, I.J. and Park, J.S. (1968) "Aneui sheet (1: 50,000)" Geol. Surv. of Korea (in Korean).

Jeong, J.G. (1980) Petrogenesis of anorthosite and related rocks in Hadong-Sancheong district, Korea. Ph.D. thesis, Seoul National University.

Jeong, J.G. (1982) Petrogenetic studies on anorthositic rocks in Hadong-Sancheong district, Korea. J. Geol. Soc. Korea, 18, 83-108.

Jeong, J.G. and Lee, Sang-man (1986) Regional metamorphism of anorthositic rocks in Hadong-Sancheong area. in Memoirs for Prof. S.M. Lee's 60th Birthday, 87-106 (in Korean).

Jeong, J.G. (1987) Magmatic differentiation of the anorthositic rocks in Hadong-Sancheong area. J. Geol. Soc. Korea, 23, 216-228 (in Korean).

Kim, O.J., Hong, M.S., Park, H.I., Park, Y.D., Kim, K.T. and Yoon, S. (1964) "Sancheong sheet (1: 50,000)" Geol. Surv. of Korea (in Korean).

Kwon, S.T. and Jeong, J.G. (1990) Preliminary Sr-Nd isotope study of the Hadong-Sancheong anorthositic rocks in Korea: Implication for their origin and for the Precambrian tectonics. J. Geol. Soc. Korea, 26, 341-349.

Lee, S.M. (1991) Variation of rock phases by the magmatic differentiation of anorthositic rocks in the area of Sanchung-eup, Sanchung-gun. M.S. thesis, Chungnam National University (in Korean).

Letteney, C.D. (1968) The anorthosite-norite-charnockite series of the Thirteenth Lake dome, South-central Adirondacks. Second Annual George H. Hudson Symposium 1966, 18, 329-342.

Mason, B. and Moore, C.B. (1982) Principles of Geochemistry (4th edition). John Wiley and Sons.

Morse, S.A. (1968) Layered intrusion and anorthosite genesis. Second Annual George H. Hudson Symposium 1966, 18, 175-187.

Nakamura, N. (1974) Determination of REE, Ba, Fe, Mg, Na and K in carbonaceous and ordinary meteorites. Geochim. Cosmochim. Acta., 38, 757-775.

Olmsted, J.F. (1968) Petrology of the Mineral Lake Intrusion, Northwestern Wisconsin. Second Annual George H. Hudson Symposium 1966, 18, 149-161.

Putman, G.W. and Burnham, C.W. (1963) Trace elements in igneous rocks, North western and Central Arizona. Geochimica et Cosmochimica acta, 27, 53-106.

Son, C.M. and Jeong, J.G. (1972) On the origin of anorthosite in the area of Hadong-Sancheong district, Kyeongsangnam-do, Korea. J. Kor. Inst. Mining Geol., 5, 1-20 (in Korean).

Wager, L.R. and Brown, G.M. (1967) Layered Igneous Rocks. W.H. Freeman and company.